AFRL-AFOSR-VA-TR-2019-0337

Design of Multifunctional Films

Ioannis Chasiotis
UNIVERSITY OF ILLINOIS

11/06/2019
Final Report

Air Force Research Laboratory
AF Office Of Scientific Research (AFOSR)/ RTB2
Arlington, Virginia 22203
Air Force Materiel Command

DISTRIBUTION A: Distribution approved for public release.

REPORT DOCUMENTATION PAGE

Form Approved
OMB No. 0704-0188

1. REPORT DATE *(DD-MM-YYYY)*	2. REPORT TYPE	3. DATES COVERED *(From - To)*
15-11-2019	Final Performance	15 Sep 2015 to 14 Sep 2018

4. TITLE AND SUBTITLE
Design of Multifunctional Films

5a. CONTRACT NUMBER

5b. GRANT NUMBER
FA9550-15-1-0470

5c. PROGRAM ELEMENT NUMBER
61102F

6. AUTHOR(S)
Ioannis Chasiotis

5d. PROJECT NUMBER

5e. TASK NUMBER

5f. WORK UNIT NUMBER

7. PERFORMING ORGANIZATION NAME(S) AND ADDRESS(ES)
UNIVERSITY OF ILLINOIS
506 S WRIGHT STREET SUITE 364
URBANA, IL 61801-3649 US

8. PERFORMING ORGANIZATION REPORT NUMBER

9. SPONSORING/MONITORING AGENCY NAME(S) AND ADDRESS(ES)
AF Office of Scientific Research
875 N. Randolph St. Room 3112
Arlington, VA 22203

10. SPONSOR/MONITOR'S ACRONYM(S)
AFRL/AFOSR RTB2

11. SPONSOR/MONITOR'S REPORT NUMBER(S)
AFRL-AFOSR-VA-TR-2019-0337

12. DISTRIBUTION/AVAILABILITY STATEMENT
A DISTRIBUTION UNLIMITED: PB Public Release

13. SUPPLEMENTARY NOTES

14. ABSTRACT

In this reporting period, the use of a compliant interphase to reduce strain transfer from a composite laminate substrate to a fully bonded photovoltaic (PV) film was investigated. Research conducted in a prior AFOSR-sponsored project (FA9550-12-1-0209) had shown that a thin film photovoltaic undergoes fragmentation and loss of its energy harvesting performance when the tensile strain in the underlying composite exceeds 0.8%. In this study, a detailed analytical model was adopted from literature to determine the required thickness and elastic modulus of an interface material that would provide strain attenuation between a unidirectional carbon fiber composite laminate and a commercial PV film. For the given properties of the composite laminate and the PV films at hand, the model pointed to the need for a very compliant layer with tens of microns in thickness and modulus of the order of 0.1 MPa. These conditions could not be met by the nanospring films developed in earlier stages of this project, which are more appropriate for strain management in microelectronics devices. Instead, we employed a compliant PDMS interphase whose effective stiffness was controlled via its elastic modulus and thickness. It was shown that such an interphase guaranteed perfect bonding of the PV film onto the composite laminate while fully attenuating the strain applied from the composite to the PV film and also maintaining the original energy harvesting performance of the PV film until tensile failure of the composite.

15. SUBJECT TERMS
Multifunctional Composites, Compliant Interface, Nanospring Films, Glancing Angle Deposition

16. SECURITY CLASSIFICATION OF:			17. LIMITATION OF ABSTRACT	18. NUMBER OF

a. REPORT	b. ABSTRACT	c. THIS PAGE		PAGES	19a. NAME OF RESPONSIBLE PERSON
Unclassified	Unclassified	Unclassified	UU		LEE, BYUNG
					19b. TELEPHONE NUMBER *(Include area code)* 703-696-8483

UNIVERSITY OF ILLINOIS
AEROSPACE ENGINEERING

Final Performance Report

Reporting Period: 09/15/2018 - 03/14/2019

Design of Multifunctional Films

PI: Ioannis Chasiotis

Aerospace Engineering
University of Illinois at Urbana-Champaign

Talbot Lab, 104 S. Wright Street, Urbana, IL 61801

Telephone: (217) 244-1474, Fax: (217) 244-0720, E-mail: chasioti@illinois.edu

AFOSR Grant # FA9550-15-1-0470

Program Manager: Dr. B.L. "Les" Lee

November 5, 2019

REPORT DOCUMENTATION PAGE

Form Approved
OMB No. 0704-0188

1. REPORT DATE *(DD-MM-YYYY)*	**2. REPORT TYPE**	**3. DATES COVERED** *(From - To)*
11/05/2019	FINAL PERFORMANCE REPORT	09/15/2018 - 03/14/2019

4. TITLE AND SUBTITLE

Design of Multifunctional Films

5a. CONTRACT NUMBER

5b. GRANT NUMBER
FA9550-15-1-0470

5c. PROGRAM ELEMENT NUMBER

6. AUTHOR(S) IOANNIS CHASIOTIS

Aerospace Engineering, U. Illinois at Urbana-Champaign, M/C 236
306 Talbot Lab, 104 South Wright St., Urbana, IL 61801

5d. PROJECT NUMBER

5e. TASK NUMBER

5f. WORK UNIT NUMBER

7. PERFORMING ORGANIZATION NAME(S) AND ADDRESS(ES)

UNIVERSITY OF ILLINOIS
Aerospace Engineering
104 South Wright St.
Urbana, IL 61801

8. PERFORMING ORGANIZATION REPORT NUMBER

9. SPONSORING / MONITORING AGENCY NAME(S) AND ADDRESS(ES)

Air Force Office of
Scientific Research (AFOSR)
Program: Mechanics of
Multifunctional Materials and
Microsystems

10. SPONSOR/MONITOR'S ACRONYM(S)
Program Manager:
Dr. B.L. Lee

11. SPONSOR/MONITOR'S REPORT NUMBER(S)

12. DISTRIBUTION / AVAILABILITY STATEMENT

Approved for public release

13. SUPPLEMENTARY NOTES

14. ABSTRACT

In this reporting period, the use of a compliant interphase to reduce strain transfer from a composite laminate substrate to a fully bonded photovoltaic (PV) film was investigated. Research conducted in a prior AFOSR-sponsored project (FA9550-12-1-0209) had shown that a thin film photovoltaic undergoes fragmentation and loss of its energy harvesting performance when the tensile strain in the underlying composite exceeds 0.8%. In this study, a detailed analytical model was adopted from literature to determine the required thickness and elastic modulus of an interface material that would provide strain attenuation between a unidirectional carbon fiber composite laminate and a commercial PV film. For the given properties of the composite laminate and the PV films at hand, the model pointed to the need for a very compliant layer with tens of microns in thickness and modulus of the order of 0.1 MPa. These conditions could not be met by the nanospring films developed in earlier stages of this project, which are more appropriate for strain management in microelectronics devices. Instead, we employed a compliant PDMS interphase whose effective stiffness was controlled via its elastic modulus and thickness. It was shown that such an interphase guaranteed perfect bonding of the PV film onto the composite laminate while fully attenuating the strain applied from the composite to the PV film and also maintaining the original energy harvesting performance of the PV film until tensile failure of the composite.

15. SUBJECT TERMS
Compliant interfaces, interphases, stress control, strain control

16. SECURITY CLASSIFICATION OF:			**17. LIMITATION OF ABSTRACT**	**18. NUMBER OF PAGES**	**19a. NAME OF RESPONSIBLE PERSON** Ioannis Chasiotis
a. REPORT unclassified	**b. ABSTRACT** unclassified	**c. THIS PAGE** unclassified		23	**19b. TELEPHONE NUMBER** *(include area code) (217) –244-1474*

Standard Form 298 (Rev. 8-98)
Prescribed by ANSI Std. Z39.18

Acknowledgements

The PI and his graduate students gratefully acknowledge the support by the Air Force Office of Scientific Research (AFOSR) through grant FA9550-15-1-0470 with Dr. B.L. Lee as the program manager.

Publications

The research results from this grant have appeared in the following publications:

D. Antartis, H. Wang, J. Wang, S. J. Dillon, H.B. Chew, I. Chasiotis, "Nanofibrillar Si Helices for Low-Stress, High-Capacity Li^+ Anodes with Large Affine Deformations,", *ACS Applied Materials and Interfaces* 11, 11715−11721, (2019).

D. Antartis, R. Mott, I. Chasiotis, "Si Nanospring Films for Compliant Interfaces," *Journal of Materials Science* 53(8), pp. 5826-5844, (2018).

D. Antartis, R. Mott, D. Das, D. Shaddock, I. Chasiotis, "Cu Nanospring Films for Advanced Nanothermal Interfaces", *Advanced Engineering Materials* 20(3), pp. 1700910(1-6), (2018).

D. Antartis, I. Chasiotis, "Individual Helical Nanostructures for Ultra-compliant Interfaces", *Materials and Design* 144, pp. 182-191, (2018).

The following manuscript has been prepared with results from the work done during the reporting period (6 months of NCE):

K-K. Hung, I. Chasiotis, "Control of Substrate Strain Transfer in Integrated Composite Laminate Structures", to be submitted to *Composites Science and Technology*, (2019).

FINAL TECHNICAL REPORT

This Final Progress Report summarizes the research conducted during the six months of no cost extension (NCE) of this grant. The research performed in the preceding three years of this project was described in detail in the three Annual Progress Reports submitted in the past.

I. NOMENCLATURE

Notation	Description
$\sigma_{S,}\sigma_{I,}\sigma_{C,}$	Stress
$\tau_{S,}\tau_{I,}\tau_{C}$	Shear Stress
$E_{1,}E_{2,}E_{3,}$	Elastic Modulus
$G_{1,}G_{2,}G_{3,}$	Shear Modulus
$\mu_{1,}\mu_{2,}\mu_{3,}$	Poisson's Ratio
L	Length of Structure
$t_{1,}t_{2,}t_{3}$	Thickness of a Layer
s	Applied Stress
$\varepsilon_{S,}\varepsilon_{I,}\varepsilon_{C}$	Strain
V	Voltage
I	Current
I_o	Reverse Diode Saturation Current
γ	Dioxide Factor
T	Absolute Temperature
e	Magnitude of Electronic Charge
I_{sc}	Short Circuit Current
V_{oc}	Open Circuit Voltage
I_{mp}	Current at Maximum Power
V_{mp}	Voltage at Maximum Power

S, I, and C stand for the PV film, the interface material, and the composite respectively.

1, 2, and 3 stand for the bottom (composite) layer, the interface material, and the top (PV film) layer, respectively.

II. INTRODUCTION

Photovoltaic (PV) thin film cells provide the means to lightweight and versatile renewable energy for a variety of applications in the aerospace industry [1]. PV films have been integrated onto load-bearing components of aerospace vehicles, satellites, and portable devices [2,3]. As a result, they are subjected to the same strains as the underlying substrate which could lead to damage and performance degradation of the brittle thin amorphous Si (aSi) film comprising a PV. The performance of PV films has been shown to degrade when subjected to relatively small strains [2-5], as demonstrated by the reduction of the fill factor (ratio of maximum power between ideal and practical conditions). Jones et al [6] reported the onset of the decline of the fill factor at ~0.75% tensile strain when the films were subjected to bending. Antartis et al [4] integrated aSi PV films with composite laminates, and showed that degradation of the fill factor begins at a substrate tensile strain of 0.8%, both for cross-ply and ±45º laminates. Fragmentation of the aSi layer was the cause of performance degradation.

While several studies have focused on improving the efficiency of PV films [7,8], there has been no study on averting their performance degradation due to substrate induced strain. The research carried out in the reporting period focused on the use of a strain attenuation interlayer between a PV film and its substrate to extend the maximum strain applied to the underlying substrate before the fill factor begins to decline and microcracking occurs in the PV film. This strain isolation concept, albeit not new, has been applied to stretchable substrates [9-12]: Lacour et al [9] used a compliant PDMS substrate to apply 25% macroscale strain while a delicate device on the substrate was exposed to only 5% strain due to its isolation by a stiff island on the substrate. In the case of PVs integrated with composite load-bearing structures, the underlying composite laminate substrate has high elastic modulus [2,3] of the order of 70-200 GPa [13]. In such cases strain isolation can be accomplished with the aid of a compliant interface material.

The main focus of this project was the development of compliant interphase layer for multifunctional applications, by glancing angle deposition (GLAD) of coiled or chevron type thin films of metals or ceramics with low shear and normal stiffness. During this project this method was successfully applied to generate compliant films of lithium ion anodes and thermal interface materials [14-17]. For instance, we employed 10-μm thick Cu nanospring films as a thermal interface material, with 25 MPa and 100 MPa shear and normal stiffness, respectively

[16]. GLAD films have the advantage of low deposition temperature, strong bonding to substrate and easy integration to next level via flat capping layers [16,18]. However, GLAD can be limited in terms of film height; the thickest GLAD films reported to date have been only 10 μm. Furthermore, a smooth substrate is needed to grow GLAD films with accurate geometrical features. Therefore, their growth as strain attenuation layers on common composite laminates was not proven practical. During the NCE period of this project (September 2018 - March 2019) we investigated the use of a compliant interphase between a PV and a unidirectional composite laminate (serving as the substrate) to provide partial or complete strain isolation of the PV. A three layer model was adopted from literature [19] to evaluate the parameter space (material properties and film thicknesses) and identify the optimal solution. Important considerations were the ability for direct process integration in large areas, rapid curing, strong adhesion, and versatility in controlling the elastic modulus.

III. MATERIALS AND METHODS

III.1 Analytical Problem Formulation

An interface material is introduced between a PV film and a unidirectional composite laminate to attenuate the strain tramistted from the composite substrate to the PV. The stress and strain fields in the stacking shown in Figure 1, were solved analytically following the solution by Li et al [19]. Since the lateral dimensions of the specimens were several orders of magnitude larger than the thickness of the PV film, the composite and the interface materials, plane strain conditions were assumed, and structural bending was neglected. Perfect bonding between layers was assumed and all materials were treated as linearly elastic in the particular loading range.

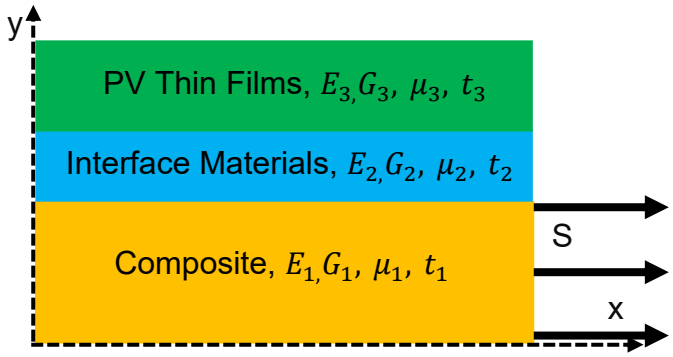

Figure 1. Schematic of (symmetric half) three layer structure.

For completeness, herein we present the problem solution methodology as reported in [19]. Based on the above assumptions and the symmetry conditions, the boundary conditions are:

$$\begin{cases} \tau_{yx}^{\mathrm{C}}\big|_{x=0} = 0, \tau_{yx}^{\mathrm{C}}\big|_{y=0} = 0 \\ \sigma_{yy}^{\mathrm{S}}\big|_{y=t_1+t_{2+}t_3} = 0 \\ \int_0^{t_1} \sigma_{xx}^{\mathrm{C}}\Big|_{x=\frac{L}{2}} dy = St_1 \\ \int_{t_1}^{t_1+t_2} \sigma_{xx}^{I}\Big|_{x=\frac{L}{2}} dy + \int_{t_1+t_2}^{t_1+t_2+t_3} \sigma_{xx}^{S}\Big|_{x=\frac{L}{2}} dy = 0 \end{cases} \quad (1)$$

An analytical solution can be obtained for the stress fields in the first layer (composite):

$$\begin{cases} \tau_{yx}^{\mathrm{C}} = P_1 sinhn_1 x sinb_1 y \\ \sigma_{xx}^{\mathrm{C}} = \frac{P_1 b_1}{n_1} coshn_1 x cosb_1 y + E \\ \sigma_{yy}^{\mathrm{C}} = -\frac{P_1 n_1}{b_1} coshn_1 x cosb_1 y + h_1(x) \end{cases} \quad (2)$$

The stress fields in the second layer (interface material) are:

$$\begin{cases} \tau_{yx}^{\mathrm{I}} = sinhn_2 x(Msinb_2 y + Ncosb_2 y) \\ \sigma_{xx}^{\mathrm{I}} = \frac{b_2}{n_2} coshn_2 x(Mcosb_2 y - Nsinb_2 y) + F \\ \sigma_{yy}^{\mathrm{I}} = -\frac{n_2}{b_2} coshn_2 x(Mcosb_2 y - Nsinb_2 y) + h_2(x) \end{cases} \quad (3)$$

The stress fields in the third layer (PV film) are:

$$\begin{cases} \tau_{yx}^{\mathrm{S}} = P_3 sinhn_3 x sinb_3(t_1 + t_2 + t_3 - y) \\ \sigma_{xx}^{\mathrm{S}} = -\frac{P_3 b_3}{n_3} coshn_3 x cosb_3(t_1 + t_2 + t_3 - y) + G \\ \sigma_{yy}^{\mathrm{S}} = \frac{P_3 n_3}{b_3} coshn_3 x cosb_3(t_1 + t_2 + t_3 - y) + h_3(x) \end{cases} \quad (4)$$

The strain in each layer in the loading direction (x direction) is:

$$\begin{cases} \varepsilon_{xx}^{\mathrm{C}} = \left(\dfrac{P_1 b_1}{n_1} coshn_1 x cosb_1 y + E - \mu_1^* \left(-\dfrac{P_1 n_1}{b_1} coshn_1 x cosb_1 y + h_1(x)\right)\right)\dfrac{1}{E_1^*} \\ \varepsilon_{xx}^{\mathrm{I}} = (\dfrac{b_2}{n_2} coshn_2 x(Mcosb_2 y - Nsinb_2 y) + F \\ -\mu_2^* \left(-\dfrac{n_2}{b_2} coshn_2 x(Mcosb_2 y - Nsinb_2 y) + h_2(x)\right))\dfrac{1}{E_2^*} \\ \varepsilon_{xx}^{\mathrm{S}} = (-\dfrac{P_3 b_3}{n_3} coshn_3 x cosb_3(t_1 + t_2 + t_3 - y) + G \\ -\mu_3^* \left(\dfrac{P_3 n_3}{b_3} coshn_3 x cosb_3(t_1 + t_2 + t_3 - y) + h_3(x)\right))\dfrac{1}{E_3^*} \end{cases} \quad (5)$$

The exact forms of the parameters in the equations above can be found in [19].

The objective of this work was to identify combinations of elastic properties and thickness values for the interface layer that result in strain attenuation between the composite and the PV films.

We define strain attenuation as:

$$\Delta\varepsilon_{xx}^{\mathrm{C-S}} = \frac{\varepsilon_{xx}^{\mathrm{C}}\big|_{y=t_1} - \varepsilon_{xx}^{\mathrm{S}}\big|_{y=t_1+t_2}}{\varepsilon_{xx}^{\mathrm{C}}\big|_{y=t_1}} \quad (6)$$

For a PV film co-cured with a composite laminate without an interphase material, the problem is reduced into a plane strain problem of two perfectly bonded layers. If structural bending is neglected the boundary conditions are:

$$\begin{cases} \tau_{yx}^{\mathrm{C}}\big|_{x=0} = 0, \tau_{yx}^{\mathrm{C}}\big|_{y=0} = 0 \\ \sigma_{yy}^{\mathrm{S}}\big|_{y=t_1+t_{2+}t_3} = 0 \\ \int_0^{t_1} \sigma_{xx}^{\mathrm{C}}\Big|_{x=\frac{L}{2}} dy = St_1 \\ \int_{t_1}^{t_1+t_2} \sigma_{xx}^{S}\Big|_{x=\frac{L}{2}} dy = 0 \end{cases} \quad (7)$$

Solving Eqn. (7) yields the stress fields in the first layer (composite):

$$\begin{cases} \tau_{yx}^{C} = P_1 sinhn_1 x sinb_1 y \\ \sigma_{xx}^{C} = \dfrac{P_1 b_1}{n_1} coshn_1 x cosb_1 y + E \\ \sigma_{yy}^{C} = -\dfrac{P_1 n_1}{b_1} coshn_1 x cosb_1 y + h_1(x) \end{cases} \quad (8)$$

The stress fields in the PV layer are:

$$\begin{cases} \tau_{yx}^{S} = P_2 sinhn_2 x sinb_2 (t_1 + t_2 - y) \\ \sigma_{xx}^{S} = -\dfrac{P_2 b_2}{n_2} coshn_2 x cosb_2 (t_1 + t_2 - y) + F \\ \sigma_{yy}^{S} = \dfrac{P_2 n_2}{b_2} coshn_2 x cosb_2 (t_1 + t_2 - y) + h_2(x) \end{cases} \quad (9)$$

where E, F, $h_1(x)$, and $h_2(x)$ are integration constants.

The strain fields in the PV film and the composite are deduced from Equations (8) and (9):

$$\varepsilon_{xx}^{C} = \left(\frac{P_1 b_1}{n_1} coshn_1 x cosb_1 y + E - \mu_1^* \left(-\frac{P_1 n_1}{b_1} coshn_1 x cosb_1 y + h_1(x) \right) \right) \frac{1}{E_1^*}$$

$$\varepsilon_{xx}^{S} = \left(-\frac{P_2 b_2}{n_2} coshn_2 x cosb_2 (t_1 + t_2 - y) + F \right. \quad (10)$$

$$\left. -\mu_2^* \left(\frac{P_2 n_2}{b_2} coshn_2 x cosb_2 (t_1 + t_2 - y) + h_2(x) \right) \right) \frac{1}{E_2^*}$$

The exact form of the parameters in the equations above is reported in [19].

III.2 Materials and Methods

PDMS was selected as the interphase material due to its tunable mechanical properties. By adjusting the ratio between the silicone elastomer and the curing agent, the elastic modulus of PDMS could be varied in the range 0.1 - 3 MPa [20,21]. The broad range of mixing ratios of the elastomer over the curing agent varying from 33:1 to 5:1 enables robust control of the viscosity

and, therefore, film thickness. Control of the PDMS film thickness and modulus enables extreme combinations of laminate and PV film thickness. Furthermore, PDMS provides the following advantages: (1) Direct integration on PV films, (2) large area coverage and flat surface for direct deposition of other materials, (3) good electrical insulation, and (4) rapid and versatile curing. PDMS was synthesized by thoroughly mixing a silicone elastomer and curing agent (SYLGARD 184, Dow Corning, Midland, MI) according targeted ratios, and degasing for 25 min. The commercial PV film modules were attached to a Si wafer for spin coating at different spinning rates according to the viscosity of PDMS, and were subsequently co-cured with the unidirectional $[0°]_8$ composite on a hot plate at 80°C and for 4 hrs. The prepregs pre-cured on a hot plate at 180°C for 4 hrs under light pressure. For better adhesion, all composites were polished by a grinder-polisher (ECOMET 3, BUEHLER, Inc.) to ensure a flat surface before attached to PDMS. In the absence of an interphase layer between the PV film and the composite laminate, the PV film was co-cured directly with the prepreg resulting in good adhesion with no debonding, and strain attenuation taking place at strains as high as 1.7%. The PV films were provided by Iowa Thin Film Technologies Inc. (Ames, IA), and comprised of a 1-μm conductive ZnO layer, 1-μm aSi, a Kapton insulation and a thick substrate, totaling ~50 μm in thickness. Unidirectional $[0°]_8$ composite laminates were fabricated as the underlying substrate, and were prepared from commercial prepregs (DA 409U/G35 150 unidirectional carbon fiber, Adhesive Prepregs from Composite Manufacturers).

The elastic modulus of PDMS reached a plateau value at the maximum cross-link ratio of 5:1, therefore, PDMS with different mixing ratios (Silicone elastomer/Curing agent) from 33:1 to 5:1 was cast into long strips ($t \times w \times l = 2 \times 5 \times 19$ mm) and tested in tension. Similarly, strips of PV films that were 2×0.2 cm^2 in size were cut for mechanical testing. A speckle pattern was deposited on the PV films and the PDMS samples to measure the strain via Digital Image Correlation (DIC). Similarly, composite laminates with and without integrated PV films were tested in tension. A speckle pattern was deposited on the backside of the composite laminates to obtain the strain field in the laminate, while a second camera was used to obtain the strain on the co-cured PV films while also measuring the fill factor. A CCD camera with a high magnification objective was used to capture small fields of view with the inherent speckle pattern of the PV films for DIC calculations and observation of film fragmentation.

The PV film was modeled as an ideal diode assuming no losses from bulk resistance and junction leakage following the study in [22]. The total current under a constant light source is given by:

$$l\,n(I_L - I) = lnI_o + \frac{|e|V}{\gamma k_B T} \tag{11}$$

The parameters γ, V, and I_o were obtained with a circuit consisted of two multimeters and one resistance substitution box at $\frac{|e|V}{\gamma k_B T} \gg 1$ and the I-V curves were plotted using via:

$$I = I_o\left[1 - \exp(\frac{|e|V}{\gamma k_B T})\right] + I_{SC} \tag{12}$$

The fill factor that quantifies the performance of PV films is defined as:

$$FF = \frac{I_{mp}V_{mp}}{I_{sc}V_{oc}} \tag{13}$$

where I_{mp} and V_{mp} correspond to the voltage and current on the I-V curve at the practical maximum power. The fill factor was measured for as-received PV films and after they were integrated onto a laminate and subjected to strain to monitor the quality of processing.

IV. RESULTS AND DISCUSSION

The stress-strain curves of the PV films and the composite laminate are shown in Figures 2(a) and 2(b), respectively, resulting in elastic moduli of 10.4 GPa and 82.8 GPa, respectively. The strain attenuation in PV films directly integrated with the composite without and interphase material, was calculated by Equation (6) at $y=t_1$ and $y=t_1+t_2$. Figure 2(c) shows no strain attenuation except for an edge effect originating in the problem solution. This is due to the fact that the effective stiffness, the product of the elastic modulus and layer thickness, of the composite is several orders of magnitude larger than that of the PV film.

A compliant interphase can provide strain attenuation by accommodating the deformation induced by the composite laminate to create a through-the-thickness gradient of the applied strain. The requisite effective compliance of such an interface material depends on the effective stiffness of the underlying composite laminate and the PV film. Different ratios of the relative effective stiffness of PV film over the composite laminate were examined. The interface material

provides the shear coupling between the laminate and the PV film, and, therefore, its effective shear compliance is proportional to its thickness and inversely proportional to the elastic modulus. Therefore, the ratio elastic modulus/thickness was used as the control parameter in the design of the appropriate PDMS interface for the materials at hand.

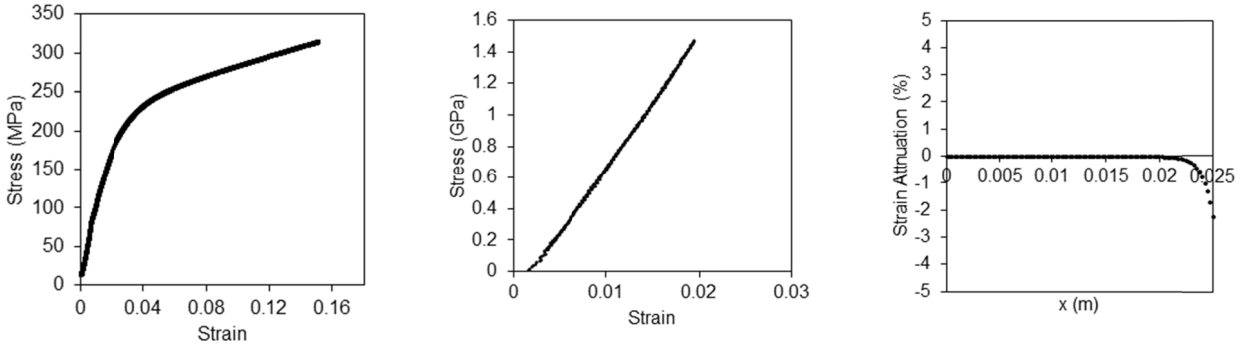

(a) **(b)** **(c)**

Figure 2. Stress-strain curve of **(a)** PV thin film modules **(b)** composite laminate, **(c)** Strain attenuation PV film integrated with the composite without an interphase material.

The material properties of the composite and the PV film, Table 1, were used as a starting point to calculate the strain attenuation through the thickness of the PDMS layer, namely at locations $y=t_1$ and $y=t_1+t_2$. The Poisson's ratio of PDMS was assumed to be 0.499. The ratio E_3t_3/E_1t_1 was varied from 0.0002 to 0.2 by changing E_3, and the modulus/thickness ratio of the interface material was calculated to obtain strain attenuation values between 0% and 100%. It was found that for a higher ratio of E_3t_3/E_1t_1, namely a stiffer PV film, a higher value of E_2/t_2 is required to achieve the same strain attenuation. For the materials at hand, $E_3t_3/E_1t_1=0.002$, as calculated from the values in Table 1 for the present case composite laminate and PV film, Figure 3 shows the strain attenuation for different ratios of E_2/t_2. For instance, for E_2/t_2 values between 2-14 MPa/mm, a strain attenuation value between 20-70% can be achieved, namely the PV film will be subjected between 80 and 30% of the strain applied to the composite laminate. Nearly 100% strain attenuation is perfectly feasible and is demonstrated herein.

Table 1. Properties of PV film and composite laminate.

	Thickness (μm)	Elastic Modulus (GPa)	Poisson's Ratio
PV film (including supporting layer)	52	10.4	0.3
Composite laminate	1900	$E_1 = 82.8$	$\nu_{12} = 0.223$

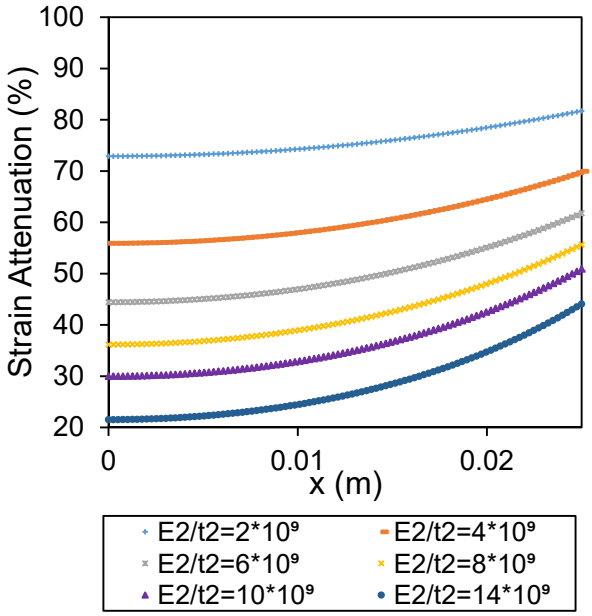

Figure 3. Strain attenuation for $E_3t_3/E_1t_1 = 0.002$. The units of E_2/t_2 are MPa/mm.

IV.1 Strain Attenuation in PDMS Layer

PDMS interface layers with various elastic moduli and thicknesses were fabricated and tested to study the possible tunability of the interface compliance. The stress vs. strain curves of PDMS for different mixing ratios of the silicone elastomer and the curing agent are shown in Figure 4(a). The relevant elastic modulus of PDMS was determined by linear fitting in a range of strains lower than 1.7%, which was the largest strain sustained by the composite laminate, and varied from 0.1 to 0.8 MPa, Table 2. . The correlation between PDMS thickness and spin-coating

rotational speed for different mixing ratios of PDMS was also determined as shown in Figure 4(b). Table 2 lists the different types of PDMS layers prepared for the purposes of this work, with E_2/t_2 values in the range 1 - 50 MPa/mm.

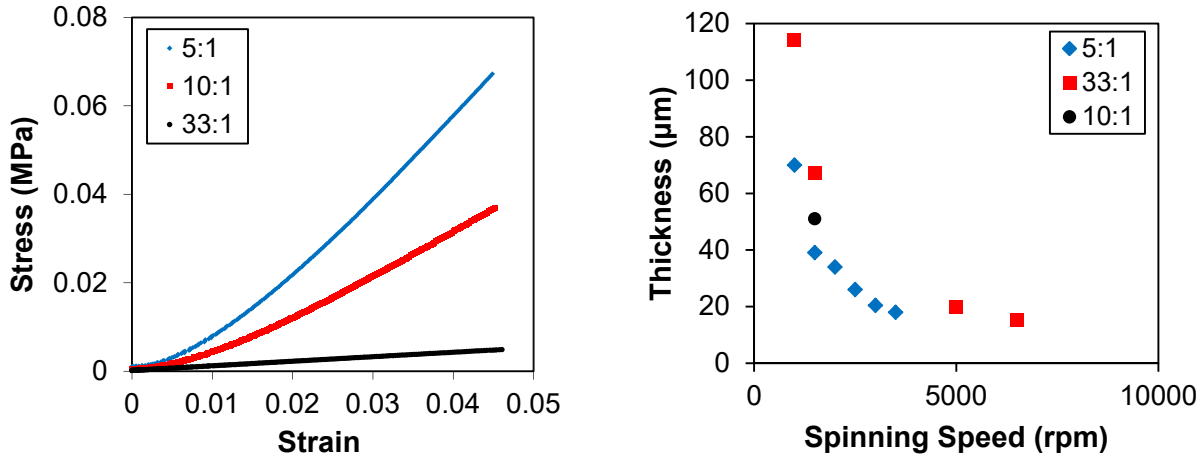

(a) **(b)**

Figure 4. (a) Stress vs. strain curves of PDMS with different mixing ratios of the silicone elastomer and the curing agent. **(b)** Speed vs. thickness correlation for PDMS with different mixing ratios.

Table 2. Elastic modulus of PDMS for different mixing ratios.

Mixing ratio (Silicone elastomer/Curing agent)	**Elastic Modulus (MPa)**
5:1	0.87
10:1	0.46
33:1	0.1

In the absence of an interface material, the composites were loaded up to 1.58% strain with practically zero measured strain attenuation, which confirmed that the deformation applied to the composite was fully transferred to the PV film. Figure 5 shows that fragmentation of the

PV film initiated at ~0.8% strain and soon saturated in terms of fragment size, which agrees with the report in [4].

Table 2. Strain attenuation for different PDMS compositions.

	$PDMS_1$	**$PDMS_2$**	**$PDMS_3$**	**$PDMS_4$**	**$PDMS_5$**	**$PDMS_6$**	**$PDMS_7$**	**$PDMS_8$**	**$PDMS_9$**
Mixing ratio (Silicone elastomer/Curing agent)	33:1	33:1	33:1	10:1	5:1	5:1	5:1	5:1	5:1
Thickness (μm)	114	67	15	51	69	39	34	26	18
Strain attenuation (%)	100	100	100	81	67	58	52	45	36

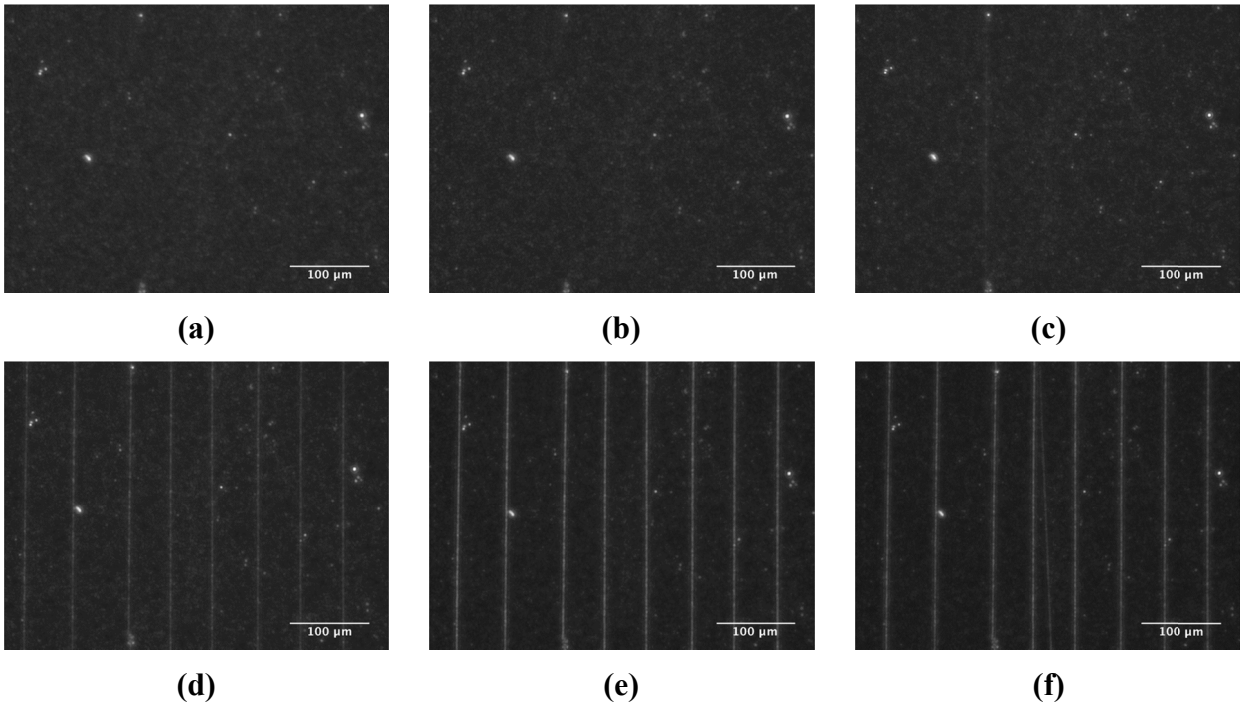

(a) **(b)** **(c)**

(d) **(e)** **(f)**

Figure 5. PV film integrated on a composite and subjected to **(a)** 0%, **(b)** 0.67%, **(c)** 0.79%, **(d)** 1%, **(e)** 1.25%, and **(f)** 1.58% tensile strain. Tensile load is applied in the horizontal direction.

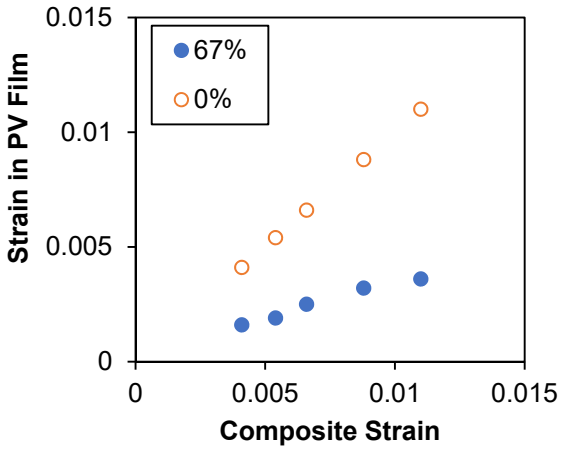

(a)

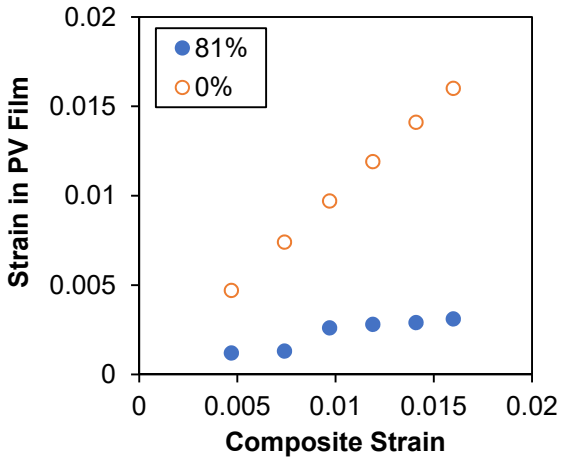

(b)

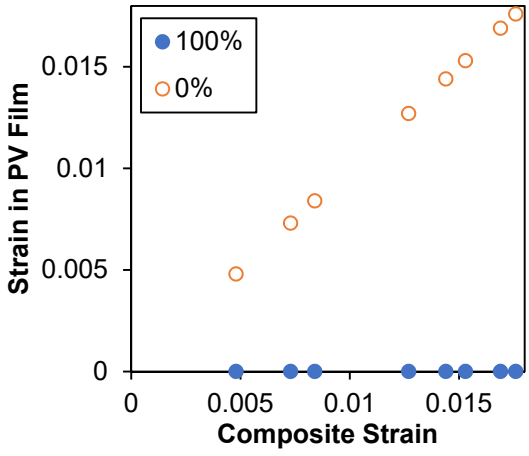

(c)

Figure 6. Tensile strain in the composite vs. the PV film (filled symbols) for strain attenuation **(a)** 67%, **(b)** 81%, and **(c)** 100%. The open symbols correspond to the strain in the PV layer in the absence of a PDMS interphase.

In the presence of a PDMS interface, the strain attenuation ranged from 36% to 100% as summarized in Table 2. Examples of the measured composite and PV film strain are given in Figure 6. The composite strain was as high as 1.76%, but the strain in the PV was as low as zero. For instance, sample $PDMS_4$ with elastic modulus of 0.46 MPa of and 51 μm thickness produced 81% strain attenuation: the strain in the composite reached 1.6% while the strain in the PV was only 0.31%, without fragmentation. Note that a post-mortem inspection showed no detachment between the PV film, the PDMS layer, or the composite.

The effective stiffness of different PDMS interfaces vs. strain attenuation is plotted in Figure 7 and compared with model predictions. The comparison shows that the model predictions provide a very conservative measure of the required effective stiffness to attain a given value of strain attenuation, often by six times. Among the possible sources for this discrepancy are the model assumptions, specifically not accounting for the effect of bending, which could lead to overestimation of the tensile strain in the PV film, since the tensile loading to the composite could induce compressive strain to the PV film due to bending, and thus reduce the overall tensile strain in the PV layer.

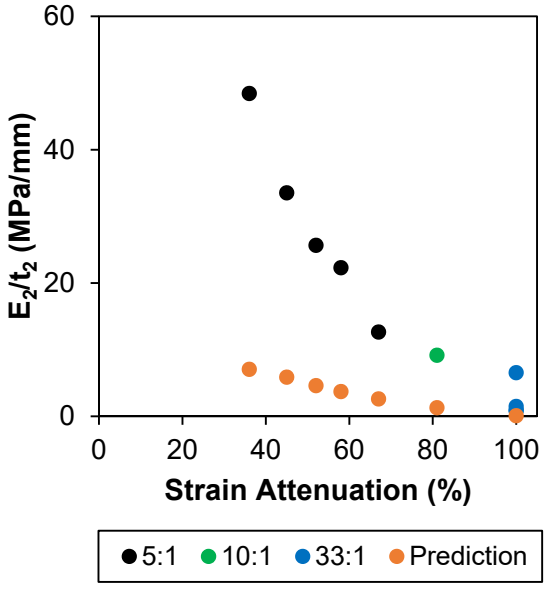

Figure 7. E_2/t_2 vs. strain attenuation.

IV.2 I-V Response vs. Composite Strain

The I-V response of the integrated PV films was measured during the entire loading process. I-V curves for different strain attenuation ratios are plotted in Figure 8. Based on these curves, the fill factors were then calculated via Equation (13) for different strains and plotted in Figure 9. In the absence of an interface material, Figure 8(a), the fill factor declined after ~0.80% strain from the initial value of 0.73 to 0.59 when the composite failed at 1.58% strain. At 0.80% strain the aSi layer also began to fragment. On the other hand, in the presence of the PDMS interface, the fill factor maintained its initial value, even when the composite strain reached values as high as 1.76%. Several examples are shown Figures 8(b-d), with the fill factor maintained at its original value of 0.7 until the composite laminate reached its tensile strength. In all these three cases, the strain in the PV layer was maintained below 0.30%.

As a final note, the effective compliance of PDMS can be tuned by changing either its thickness or the elastic modulus to reach a target ratio E_2/t_2. For instance, the elastic modulus alone could increase the strain attenuation from 36% to 100%. The versatility in the elastic modulus of PDMS allows us to address a broad range of underlining substrate and top layer combinations with a variety of values for the relative effective stiffness (E_3t_3/E_1t_1), since the ratio E_2/t_2 of the interface layer can be varied by as much as 3 orders of magnitude between 0.2 and 200 MPa/mm to achieve the desired amount of strain attenuation. While selecting the values of E_2 and t_2 additional considerations arise from the minimum possible uniform thickness of the interface layer, the roughness of the composite laminate, the maximum acceptable thickness of the interface layer, and the bounds in the elastic modulus of PDMS for different ratios of the silicone elastomer and the curing agent.

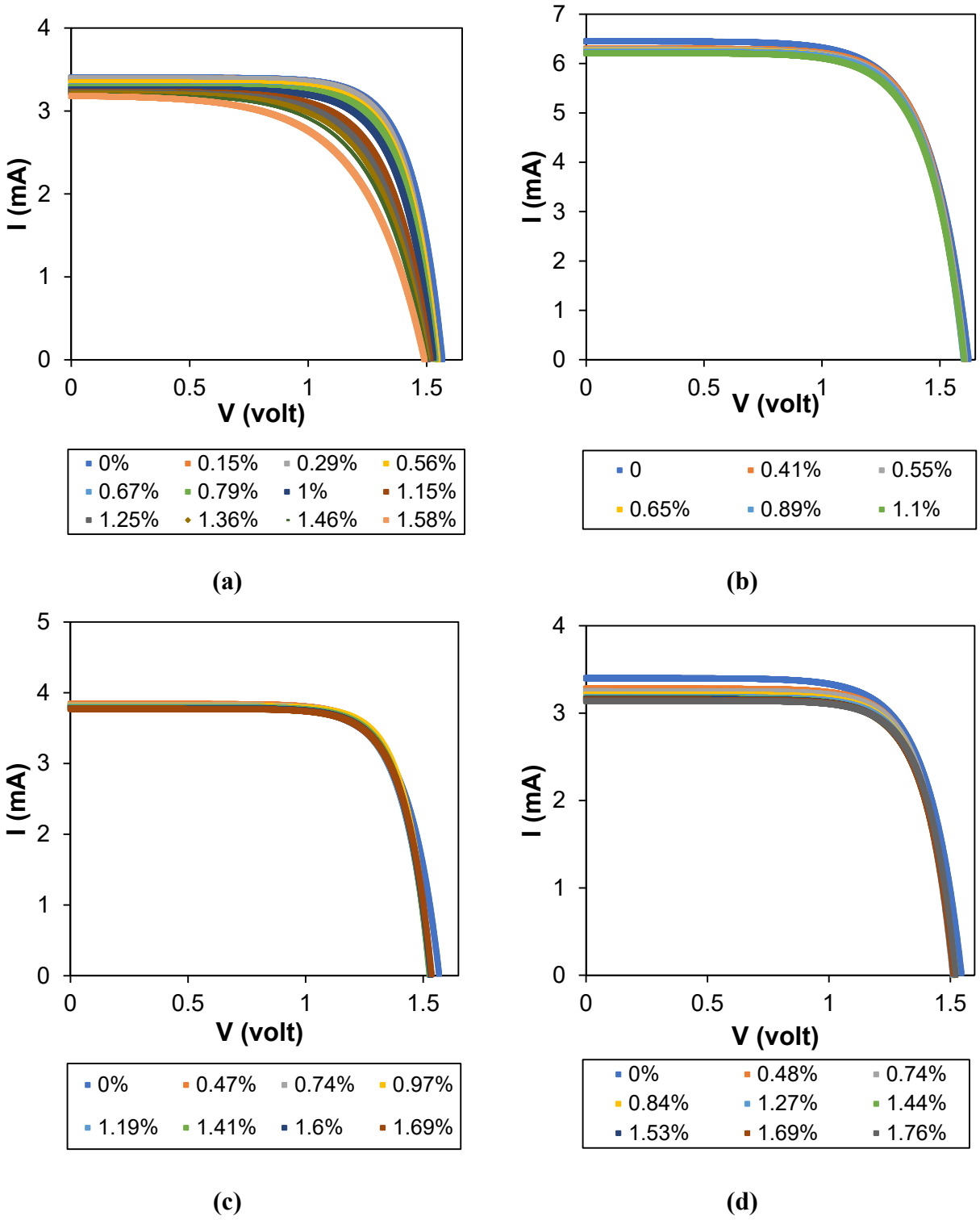

Figure 8. I-V curves of PV films with **(a)** 0%, **(b)** 67%, **(c)** 81%, and **(d)** 100% tensile strain attenuation.

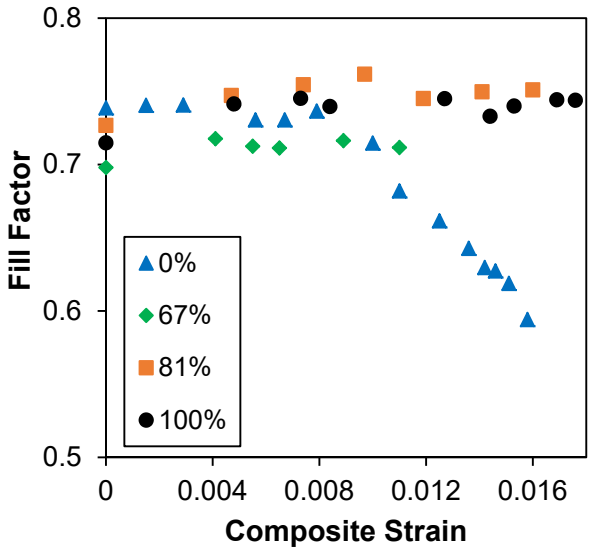

Figure 9. Fill factors of PV films under different strain attenuation values.

V. CONCLUSIONS

The introduction of an interface material to extend the maximum strain applied to a composite laminate before degradation of an integrated PV overlayer was investigated. In the absence of an interphase between the two materials, the PV layer begins to fragment at 0.80% strain, gradually losing its performance and functionality. An analytical model adopted for the purposes of this study showed that a compliant interface material provides strain attenuation that depends on its modulus-to-thickness ratio. While the model captured correctly the trends between strain attenuation and the ratio modulus-to-thickness of the interphase, it provided very conservative estimates for the required PDMS interphase. Different combinations of the elastic modulus and thickness of PDMS provided a broad range of E_2/t_2 values, from 1 to 50 MPa/mm, which were used as the control parameter to attenuate the transfer of composite strain to the PV layer by as much as 100%. As a result, the fill factor of the PV films maintained its high value until composite failure at 1.76% strain, whereas in the absence of PDMS the fill factor declined beyond 0.8% strain in the composite laminate. The work presented herein provides a framework for the design of compliant interphases in material systems with integrated functionalities, in order to control the transfer of strain/stress from a structural layer to a functional film.

VI. REFERENCES

[1] A. Reinders, P. Verlinden, W. Sark, and A. Freundlich, "Photovoltaic Solar Energy: from fundamentals to applications." *Chichester: Wiley*, (2007).

[2] K. J. Maung, H. T. Hahn, and Y. Ju, "Multifunctional integration of thin-film silicon solar cells on carbon-fiber-reinforced epoxy composites." *Solar Energy, 84(3)*, pp. 450, (2010).

[3] G. Dennler, S. Bereznev, D. Fichou, K. Holl, D. Ilic, R. Koeppe, …,and T. Wöhrle, "A self-rechargeable and flexible polymer solar battery." *Solar Energy, 81(8)*, pp. 947, (2007).

[4] D. Antartis, and I. Chasiotis, "Residual stress and mechanical property measurements in amorphous Si photovoltaic thin films." *Solar Energy, 105,* pp. 694-704, (2014).

[5] J. C. Kim, and S. K. Cheong, "I–V curve characteristics of solar cells on composite substrate under mechanical loading." *Journal of Mechanical Science and Technology, 28(5)*, pp. 1694, (2014).

[6] R. Jones, T. Johnson, W. Jordan, S. Wagner, J. Yang, and S. Guha, "Effects of mechanical strain on the performance of amorphous silicon triple-junction solar cells." *Conference Record of the Twenty-Ninth IEEE Photovoltaic Specialists Conference*, pp. 1214, (2002)

[7] J. Park, V. A. Dao, S. Kim, D. P. Pham, S. Kim, A. H. Le, J. Kang, and J. Yi, "High Efficiency Inorganic/Inorganic Amorphous Silicon/Heterojunction Silicon Tandem Solar Cells." *Scientific Reports, 8(1), pp. 1*, (2018)

[8] Y. Xu, Z. Hu, H. Diao, Y. Cai, S. Zhang, X. Zeng, H. Hao, X. Liao, E. Fortunato, and R. Martins, "Heterojunction solar cells with n-type nanocrystalline silicon emitters on p-type c-Si wafers." *Journal of Non-Crystalline Solids, 352(9-20)*, pp. 1972, (2006).

[9] S. P. Lacour, S. Wagner, R. J. Narayan, T. Li, and Z. Suo, "Stiff subcircuit islands of diamond-like carbon for stretchable electronics." *Journal of Applied Physics, 100(1)*, pp. 014913-2. (2006).

[10] J. Sun, N. Lu, J. Yoon, K. Oh, Z. Suo, and J. J. Vlassak, "Inorganic islands on a highly stretchable polyimide substrate." *Journal of Materials Research, 24(11)*, pp. 3338. (2009).

[11] N. Lu, J. Yoon, and Z. Suo, "Delamination of stiff islands patterned on stretchable substrates. " *International Journal of Materials Research, 98(8)*, pp. 717, (2007).

[12] D. Kim, Y. Kim, J. Wu, Z. Liu, J. Song, H. Kim, Y. Y. Huang, K. C. Hwang and J. A. Rogers, J. A, "Flexible electronics: ultrathin silicon circuits with strain-isolation layers and mesh layouts for high-performance electronics on fabric, vinyl, leather, and paper." *Advanced Materials, 21(36)*, pp. 3704-3705, (2009).

[13] G. Lubin, "Handbook of composites." *New York: Van Nostrand Reinhold*, (1982).

[14] D. A. Antartis, R. N. Mott, and I. Chasiotis, "Si nanospring films for compliant interfaces." *Journal of Materials Science, 53(8)*, pp. 5829, (2017).

[15] D. A. Antartis, R. N. Mott, and I. Chasiotis, “Silicon nanosprings fabricated by glancing angle deposition for ultra-compliant films and interfaces.” *Materials & Design, 144*, pp. 184, (2018).

[16] D. A. Antartis, R. N., Mott, D. Das, D. Shaddock, and I. Chasiotis, “Cu Nanospring Films for Advanced Nanothermal Interfaces.” *Advanced Engineering Materials, 20(3)*, pp. 1700910–2, (2018).

[17] D. A. Antartis, H. Wang, C. Y. Tang, H. B. Chew, S. J. Dillon, and I. Chasiotis, “Nanofibrillar Si Helices for Low-Stress, High-Capacity Li Anodes with Large Affine Deformations.” *ACS Applied Materials & Interfaces, 11(12)*, PP. 11716, (2019).

[18] P. M. Martin, “Handbook of deposition technologies for films and coatings: science, applications and technology.” *Amsterdam: Elsevier*, (2010).

[19] L. Li, R. Li, S. Wang, Z. Wang, T. Ling, and C. Li, “Stress analysis of film-on-substrate structure under tensile loads.” *Mechanics of Materials, 120*, pp. 1-14, (2018).

[20] N. Evans, C. Minelli, E. Gentleman, V. Lapointe, S. Patankar, M. Kallivretaki, X. Chen, C. J. Robert, and M. Stevens,“ Substrate stiffness affects early differentiation events in embryonic stem cells. *” European Cells and Materials, 18*, pp. 4, (2009).

[21] X. Q. Brown, K. Ookawa, and J. Y. Wong, “Evaluation of polydimethylsiloxane scaffolds with physiologically-relevant elastic moduli: interplay of substrate mechanics and surface chemistry effects on vascular smooth muscle cell response.” *Biomaterials, 26(16)*, pp. 3125, (2005).

[22] M. Morgan, G. Jakovidis, and I. Mcleod. “An experiment to measure the I-V characteristics of a silicon solar cell.” *Physics Education*, *vol. 29, no. 4*, 1994, pp. 253–254, (1994).